Characteristics of the Greenhouse Gas Concentration Derived from the Ground-based FTS Spectra at Anmyeondo, Korea

Young-Suk Oh[1,2*], Samuel Takele Kenea[1], Tae-Young Goo[1], Kyu-Sun Chung[2], David W. T. Griffith[3], Voltaire A. Velazco[3], Gawon Kim[1], Jae-Sang Rhee[1], Me-Lim Oh[4], Haeyoung Lee[4], and Young-Hwa Byun[1]

1. Climate Research Division, National Institute of Meteorological Sciences (NIMS), Jeju-do, Korea
2. Department of Electrical Eng. & Center for Edge Plasma Science, Hanyang University, Seoul, Korea
3. School of Chemistry, University of Wollongong, Wollongong, Australia
4. Climate Change Monitoring Division, Korea Meteorological Administration, Seoul, Korea

*Correspondence to: Young-Suk Oh (ysoh306@korea.com)

Abstract. Since the late 1990s, the meteorological observatory established in Anmyeondo (36.5382˚ N, 126.3311˚ E, and 30 m above mean sea level), has been monitoring several greenhouse gases such as CO_2, CH_4, N_2O, CFCs, and SF_6, as part of the Global Atmosphere Watch (GAW) Program. A high resolution ground-based (g-b) Fourier Transform Spectrometer (FTS, IFS-125HR model) was installed at such observation site in 2013, and has been fully operated within the frame work of the Total Carbon Column Observing Network (TCCON) since August, 2014. The solar spectra recorded by the g-b FTS are covered in the range between 3,800 and 16,000 cm^{-1} at the spectral resolution of 0.02 cm^{-1} during the measurement period between 2013 and 2016. In this work, the GGG2014 version of the TCCON standard retrieval algorithm was used to retrieve XCO_2 concentrations from the FTS spectra. Two spectral bands (at 6220.0 and 6339.5 cm^{-1} center wavenumbers) were used to derive the XCO_2 concentration within the spectral residual of +0.01 %. All sources of errors were thoroughly analyzed. In this paper, we introduced a new home made OASIS (Operational Automatic System for Intensity of Sunray) system to our g-b FTS instrument and that allows reducing the solar intensity variations (SIV) below 2 %. A comparison of the XCO_2 concentration in g-b FTS and OCO-2 (Orbiting Carbon Observatory) satellite observations were presented only for the measurement period between 2014 and 2015. Nine coincident observations were selected on a daily mean basis. It was obtained that OCO-2 exhibited low bias with respect to the g-b FTS, which is about -0.065 ppm with the standard deviation of 1.66 ppm, and revealed a strong correlation (R=0.85). Based on seasonal cycle comparisons, both instruments generally agreed in capturing seasonal variations of the target species with its maximum and minimum values in spring and late summer, respectively.

In the future, it is planned to exert further works in utilizing the FTS measurements for the evaluation of satellite observations such as Greenhouse Gases Observing Satellite (GOSAT) at observation sites. This is the first report of the g-b FTS observations of XCO_2 species over the Anmyeondo station.

Key words: XCO_2, G-b FTS, GOSAT, TCCON, Infrared spectra, OASIS

1 Introduction

Monitoring of greenhouse gases (GHGs) is a crucial issue in the context of the global climate change. Carbon dioxide (CO_2) is one of the key greenhouse gas and its global annual mean concentration has been increased rapidly from 278 to 400 ppm since 1750, pre-industrial year (WMO greenhouse gas bulletin, 2016). Radiative forcing of atmospheric CO_2 accounts for approximately 65 % of the total radiative forcing by long-lived GHGs (Ohyama et al., 2015 and reference therein). Human activities, such as burning of fossil fuels, land use change, etc., are the primary drivers of the continuing increase in atmospheric greenhouse gases and the gases involved in their chemical production (Kiel et al., 2016 and reference therein), In the fact that it is a global concern for demanding accurate and precise long-term measurements of greenhouse gases.

In the field of remote sensing techniques, solar absorption infrared spectroscopy is an essential technique, which has been increasingly used to determine changes in atmospheric constituents. Nowadays, a number of instruments deployed in various platforms (e.g., ground-based, space-borne) have been operated for measuring GHGs such as CO_2. Our g-b FTS at the Anmyeondo station has been measuring several atmospheric GHGs operated within the framework of the Total Carbon Column Observing Network (TCCON). XCO_2 retrievals from the g-b FTS have been reported at different TCCON sites (e.g, Ohyama et al., 2009; Deutscher et al., 2010; Messerschmidt et al., 2010, 2012; Miao et al., 2013; Kivi and Heikkinen, 2016). TCCON achieves the accuracy and precision in measuring the total column of CO_2 as about 0.25 % that is less than 1 ppm (Wunch et al., 2010), which is essential to get information about sinks and sources, as well as validating satellite products (Rayner and O'Brien, 2001; Miller et al., 2007). It is reported that the precision of CO_2 even 0.1 % can be achieved during clear sky conditions (Messerschmidt et al., 2010; Deutscher et al., 2010). The network aims to improve global carbon cycle studies and to supply the primary validation data of different atmospheric trace gases derived from space-based instruments, e.g., the Orbiting Carbon Observatory 2 (OCO-2), the Greenhouse Gases Observing Satellite (GOSAT) (Frankenberg et al., 2015; Morino et al., 2011).

The objective of this study is focused on the characteristics of XCO_2 concentration retrievals from g-b FTS spectra and is to implement a preliminary comparison against OCO-2 over the Anmyeondo station. The FTS spectra have been processed using the TCCON standard GGG2014 (Wunch et al., 2015) retrieval software. One of the interesting issues in this work is that we introduce a new home made OASIS system to our g-b FTS instrument, by which we were able to attain SVI (solar intensity variations) below 2 %.

This paper is organized as follows: Sect. 2 introduces instrumentations and measurement site descriptions. Sect. 3 represents results and discussion. The conclusion is given in Sect. 4.

2 Site and instrumentation

2.1 Site description

The G-b FTS observatory was established in the Anmyeondo (AMY) station, which is located at 36.32˚ N, 126.19˚ E, and 30 m above sea level. This station is situated on the west coast of the Korean Peninsula, which is 180 kilometer away from Seoul, the capital city of Korea. Figure 1 displays the Anmyeondo station. It is also a regional GAW (Global Atmosphere Watch) station that belongs to the Climate Change Monitoring Network of KMA (Korean Meteorological Administration). The AMY station has been monitoring various atmospheric compositions such as greenhouse gases, aerosols, ultraviolet radiation, ozone, and precipitation since 1999. The total area of Anmyeondo is estimated to be ~87.96 km^2 and approximately 1.25 million people reside in this island. Some of the residents over this area are engaged in agricultural activities. The topographic feature of the area consists of low level hills, on average it is about 100 m above sea level. The climatic condition of the area is: the minimum temperature is occurred on winter season with an average of 2.7 ˚C, and the maximum temperature is about 25.6 ˚C during summer season. In addition, the annual precipitation amount is estimated to be 1,155 mm; and the high amount of snows would be observed in winter. Such observation site has been designated as part of TCCON site since August 2014. The AMY site's on TCCON wiki page is kept available and can be found at: https://tccon-wiki.Anmyeondo.edu/Sites/Anmyeondo.

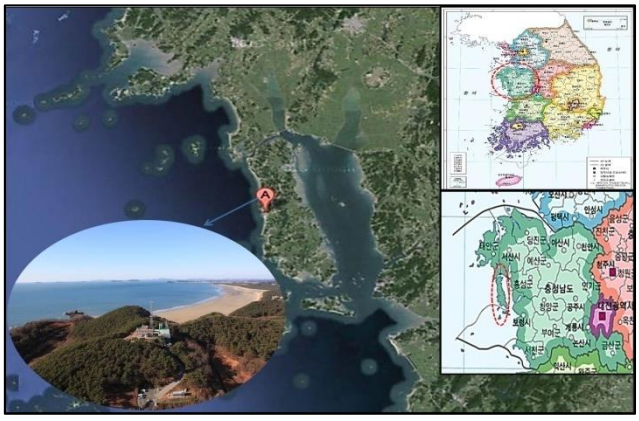

Figure 1: Anmyeondo(AMY) station

2.2 G-b FTS instrument

Solar spectra are acquired by operating a Bruker IFS 125HR spectrometer (Bruker Optics, Germany) under the framework of TCCON. Currently, our g-b FTS instrument operation is semi-automated for taking the routine measurements under clear sky conditions. It is planned to make an FTS operation mode to be fully automated by this year. The solar tracker (Tracker A 547, BrukerOptics, Germany) is mounted inside a dome. The tracking ranges in terms of both azimuthal and elevation angles are about 0˚ to 315˚ and 10˚ to 85˚ degrees, respectively, while the tracking speed is about 2 degrees per second. The tracking accuracy of ±4 minutes of arc can be achieved by the Camtracker mode. Under clear sky conditions, the dome is opened and set to an automatic-turning mode, so that the mirrors are moved

automatically to search for the position where the sunspot is seen by the camera. Then, the solar tracker is activated in such a way that the mirrors are finely and continuously controlled to fix the beam into the spectrometer. Figure 2 displays an overview of the general data acquisition system. This ensures that all spectra were recorded under clear weather conditions. The other important feature that has been made on the FTS spectrometer is the implementation of the interferogram sampling method (Brault, 1996), that takes advantage of modern analog-digital converters (ADCs) to improve the signal-to-noise ratio.

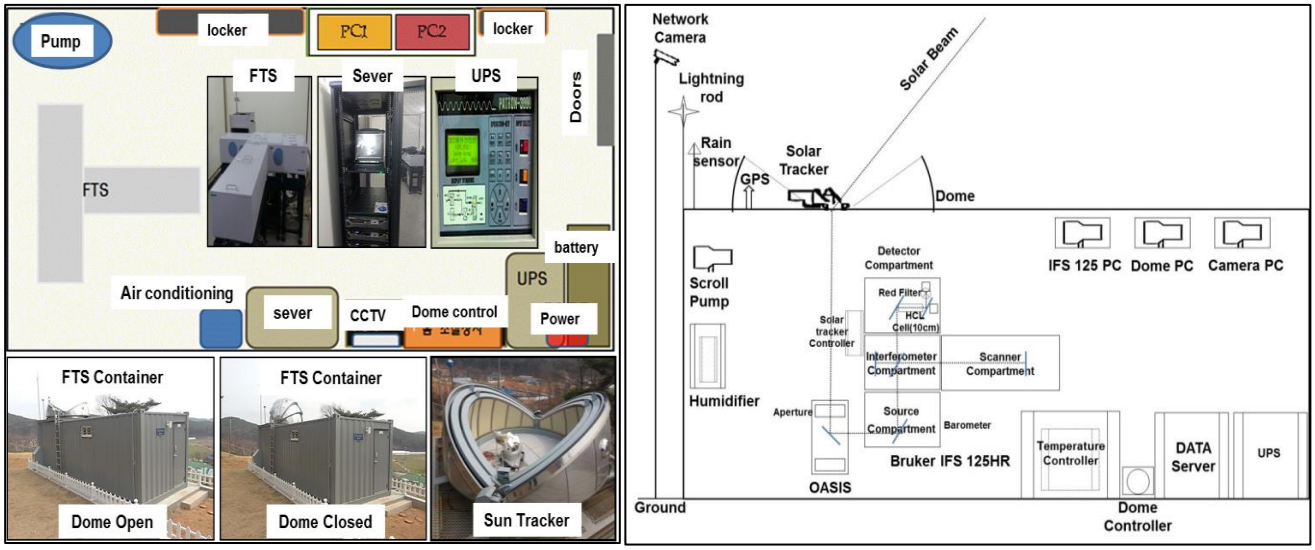

Figure 2: Photographs of the automated FTS laboratory. The Bruker Solar Tracker type A547 is mounted in the custom made dome. A servo controlled solar tracker directs the solar beam through a CaF_2 window to the FTS (125HR) in the laboratory. The server computer is used for data acquisition. PC1 (IFS 125HR), PC2 (Dome) and PC3 (Camera) are used for controlling the spectrometer, solar tracker, dome, camera, pump, GPS satellite time, and humidity sensor.

The spectrometer has equipped with two room temperature detectors; an Indium-Gallium-Arsenide (InGaAs) detector, which covers the spectral region from 3,800 to 12,800 cm^{-1}, and a Silicon (Si) diode detector (9,000 – 25,000 cm^{-1}) used in a dual-acquisition mode with a dichroic optic (Omega Optical, 10,000 cm^{-1} cut-on). A filter (Oriel Instruments 59523; 15,500 cm^{-1} cut-on) prior to the Si diode detector blocks visible light, which would otherwise be aliased into a near-infrared spectral domain. TCCON measurements are routinely recorded at a maximum optical path difference (OPD_{max}) of 45 cm leading to a spectral resolution of 0.02 cm^{-1}. Two scans, one forward and one backward, are performed and individual interferograms are recorded. A single scan in one measurement takes about 110 s. The pressure inside FTS is kept at 0.1 to 0.2 hPa with oil-free pump to maintain the stability of the system and to ensure clean and dry conditions.

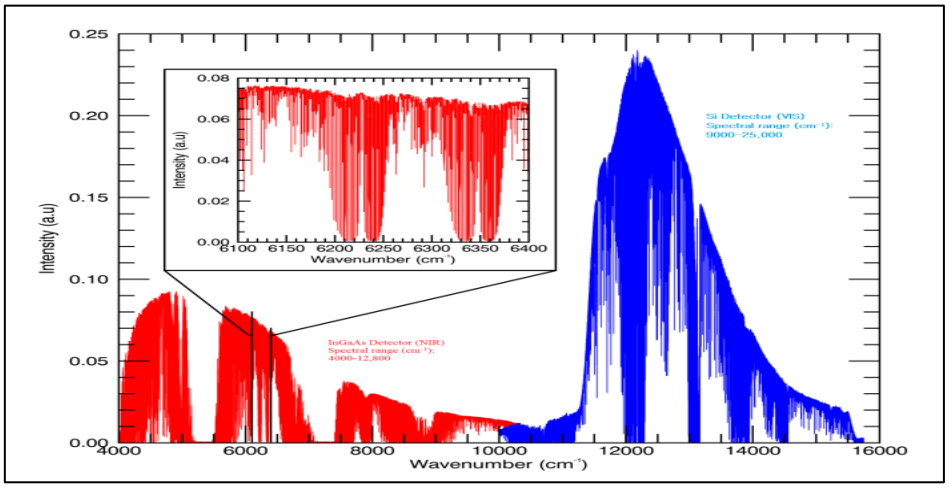

Figure 3: Single spectrum recorded on 4 October 2014 with a resolution of 0.02 cm^{-1}. Signal-to-noise ratio is ~900 for the InGaAs detector (A) and ~500 for the Si diode detector (B). A typical example for the spectrum of XCO_2 is shown in the inset.

Table 1. Measurement setting for the Anmyeondo g-b FTS spectrometer of the Bruker 125HR model

Item	Setting
Aperture	0.8 mm
Detectors	RT-Si Diode DC, RT-InGaAs DC
Beamsplitters	CaF_2
Scanner velocity	10 kHz
Low pass filter	10 kHz
High folding limit	15798.007031
Spectral Resolution	0.02 cm^{-1}
Optical path difference	45 cm
Acquisition mode	Single sided, forward-backward
Sample scan	2 Scans
Sample scan time	~110 s

2.3 Operational Automatic System for the Intensity of Sunray (OASIS)

The OASIS system is developed for improving the quality of the spectra recorded by the spectrometer. To ensure the quality of the spectra, this system is beneficial for minimizing the noise that induced in the spectra due to rapid intensity fluctuations of the incoming solar radiation that reaches to the instrument. The main function of the OASIS is to control the aperture diameter of inlet through which the incoming radiation goes to the interferometer. This aperture is placed inside the OASIS system, which is different from the actual aperture that is located inside the interferometer compartment. The aperture size varies in the range of 26 to 32 mm with respect to the photon sensor signals at the OASIS system, which is operated at voltage ranges of approximately 0 to 219 mV. Figure 4 depicts the schematic views of the OASIS systems. As can be seen in the figure, the basic components of the OASIS system such as photoelectric sensor, stepping motor, and sunray controller are shown clearly. In fact, the detail characteristic of the operation is beyond the scope of this paper. The fundamental purpose of this system is to optimize the measurement of the solar spectra by reducing the effect of the fluctuations (sudden drops) of the intensity of the incoming light occurred due to changes in thin clouds

and aerosols loads or interceptions by any other objects along the line of sight over the measurement site. The maximum threshold value of the solar intensity variation (SIV) is 5 % that is the TCCON standard value (Ohyama et al., 2015). Therefore, we have reduced this value to 2 % in our case by introducing a new home made OASIS system to our g-b FTS since December 2014. This allows us to ensure for having high quality spectra from the instrument. In this work, we have used this quality criterion to screen out the quality of the spectra. Figure 5 illustrates an example, taken on date 4 April 2015, on variations in levels of intensity with and without equipped the OASIS system to the g-b FTS instrument. It is clearly seen that the large amplitude of the solar intensity variation is filtered in the spectra. Note that the solar intensity difference was exhibited as can be seen in the figure, which was due to the measurement time difference.

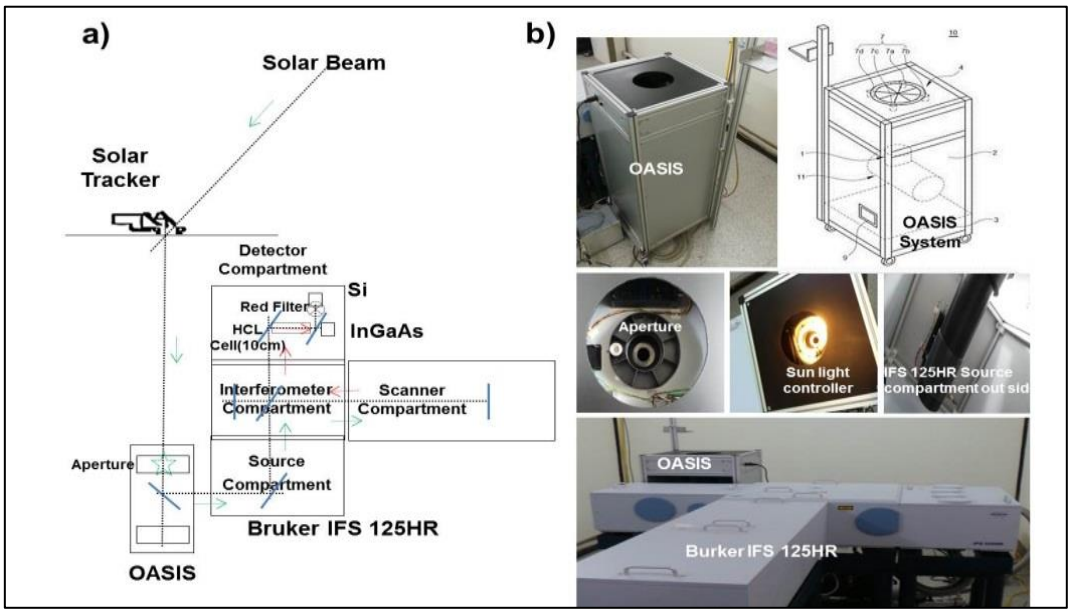

Figure 4: Schematic views of the OASIS system. a) Shows the configuration of installed equipment and movement path of solar beam, b) Shows the detailed configuration of OASIS

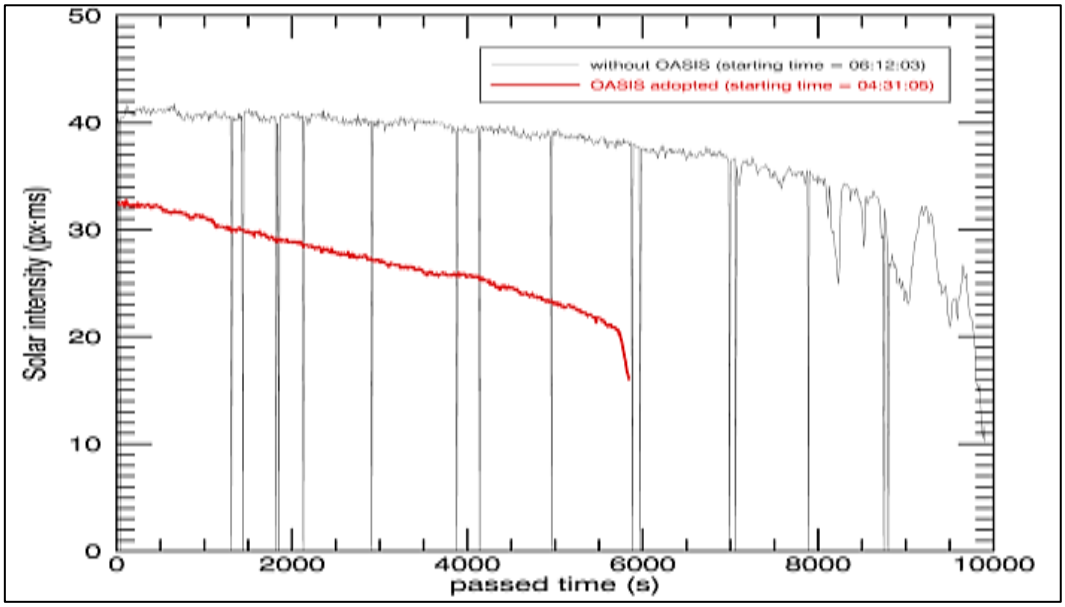

Figure 5: Typical example for solar intensity versus time with and without OASIS is given. (Taken on 04 April, 2015)

2.4 Retrieval methodology

The TCCON standard GGG2014 (version 4.8.6) (Wunch et al., 2015) retrieval software developed by JPL is used to determine the abundances of XCO_2 from the FTS spectra. Within the GGG package, there is a GFIT (version 4.37) section, which is a nonlinear least squares spectral fitting program developed for analysing FTS spectra (Messerschmidt et al., 2010; Wunch et al., 2011). GFIT is developed in such a way that its "forward model" is independent of and separable from its "inverse method". The forward model is an algorithm that computes the atmospheric spectra compared to the observed spectra, incorporating radiative transfer and molecular physics along with assumed gas distributions (Connor et al., 2016)

Table 2. Spectral windows used for the retrievals of the columns of CO_2 and O_2

Gas	Center of spectral window (cm^{-1})	Width (cm^{-1})	Interfering gas
O_2	7885.0	240.0	H_2O, HF, CO_2
CO_2	6220.0	80.0	H_2O ,HDO, CH_4
CO_2	6339.5	85.0	H_2O ,HDO

The GFIT forward model calculation uses 70 vertical levels spaced at 1 km intervals to represent the atmosphere. The CO_2 column amount is retrieved from two spectral windows centred at 6220 and 6339.5 cm^{-1} (see Table 3). The calculated and the measured spectra are compared, and the residual is minimized by iteratively scaling the gas VMR profiles (Messerschmidt et al., 2012). A typical example for the measured spectrum of CO_2 in these bands is shown in the inset of Fig. 3. The spectroscopic line parameters for the CO_2 retrieval are taken from the High Resolution Transmission data (HITRAN) 2012 (Rothman et al., 2013). The inverse method retrieves a state vector of parameters, such as volume mixing ratio of the target species, by computing values that provide a best fit to the spectrum by employing other assumptions and constraints (Connor et al., 2016). The apriori profiles generated by the TCCON retrieval algorithm are based on the National Centre for Environment Prediction (NCEP) reanalysis data (http://www.cdc.noaa.gov/data/gridded/data.ncep.reanalysis.html) for temperature, pressure, and humidity. The a priori profile of CO_2 is derived based on a model fitted to the GLOBALVIEW data.

The standard TCCON retrieval uses O_2 retrieved from the same spectra as the target gases in the band at 7885 cm^{-1} to estimate the total dry-air column. The retrieved CO_2 column is then divided by the retrieved O_2 column to compute the column average dry-air mole fraction.

$$XCO_2 = \frac{CO_{2\,\text{column}}}{O_{2\,\text{column}}} \times 0.2095\,, \qquad (1)$$

Computing the ratio using Eq. (1) minimizes systematic and correlated errors such as errors in solar zenith angle, surface pressure, and instrumental line shape that existed in the retrieved CO_2 and O_2 columns (Messerschmidt et al., 2012, Washenfelder et al., 2006). In addition, the retrieved dry-air mole

fractions were used by filtering the data points with high solar zenith angle of (> 80^{o}) (Buschmann et al., 2016).

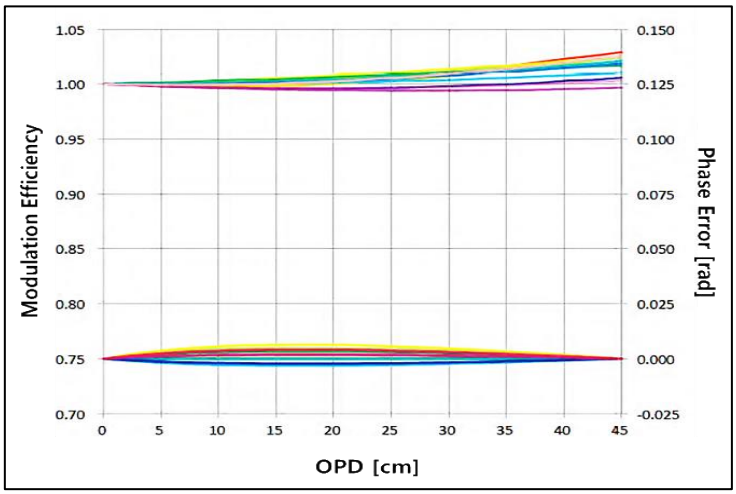

Figure 6: Modulation efficiency and phase error (rad) of HCl measurements from the g-b FTS are displayed in the period from October 2013 to September, 2014. Resolution: 0.015 cm^{-1}, Aperture: 0.8 mm, and Detector: RT-InGaAs DC (from 2013.10 (red) to 2016.09 (black)).

2.5 Characterization of FTS-instrumental line shapes

For the accurate retrieval of total column values of the species of interest, a good alignment of the g-b FTS is essential. The instrument line shape (ILS) is retrieved from the regular HCl cell measurement that is an important indicator of the status of the FTS's alignment (Hase et al., 1999). The analyses of the measurements were performed using a linefit spectrum fitting algorithm (LINFIT14 software) (Hase et al., 2013). Here, we have carried out experiments to investigate the influences of ILS with and without to the presence of OASIS system, and then we considered HCl cell measurements using sun as source while OASIS system active and tungsten lamp as a source while OASIS inactive. Without OASIS system, we showed the time series of the modulation efficiency and phase error (rad) in the HCl measurement using the source of light from tungsten lamp in the period of October 2013 to September 2016, which is depicted in Fig. 6. Modulation amplitudes for well alignment should be controlled in a limit of 5 % loss at the maximum optical difference (Wunch et al., 2011). In our g-b FTS measurements, it is found that the maximum loss of modulation efficiency at the maximum OPD is about 3 %, which is quite close to the ideal value. The phase errors are less than 0.009. Hase et al. (2013) reported that this level of small disturbances from the ideal value of the modulation efficiency is common to all well-aligned instruments. This result confirmed that the g-b FTS instrument is well aligned and stable during the whole operation period.

In the case OASIS system in active mode, we also confirmed that the ILS was not affected by the variable aperture during the operation of this system. The modulation efficiency and phase error were estimated to be 99.96 % and 0.009 rad, respectively (**see Table 3**). Sun et al. (2017) reported the detailed characteristics of the ILS with respect to applications of different optical attenuators to FTIR spectrometers within the TCCON and NDACC networks. They used both lamp and sun cell

measurements which were conducted after the insertion of five different attenuators in front of and behind the interferometer. In Sun et al. (2017) paper, the ILS result was indicated by considering optical attenuator no .1 which is in good agreement with our findings.

Table 3. ILS measurements with and without OASIS system (sources of light are tungsten lamp and solar light).

Light Source	Tungsten	Solar(Sun)	Solar(Sun)	Range
S/N (signal to noise ratio)	183.2 : 1	162.7 : 1	167.1 : 1	_
Width (cm^{-1})	0.0137	0.0143	0.0145	
Center wavenumber	5687.65 cm^{-1}	5687.65 cm^{-1}	5687.65 cm^{-1}	
Residual (measured minus simulated spectra)	-0.0005 to 0.0005	-0.001 to 0.001	-0.001 to 0.001	_
Mod. eff	99.99 %	99.98 %	99.96 %	99.96 ~99.99 %
Phase error (rad)	0.007	0.009	0.009	0.007 – 0.009
OASIS run	**OFF**	**OFF**	**ON**	_
Parameter (Spectra Observation)	**(Same)** Resolution: 0.015cm^{-1}, Scans: 50, Beamsplitter: CaF_2, Aperture: 0.8 mm, Detector: RT-InGaAs DC, Scanner velocity: 10 kHz, High pass filter: open, Low pass filter: 10kHz, Optical Path difference (OPD) = 45 cm **(Difference)** Source setting: Emission back parallel input(SUN), NIR(Tungsten)			

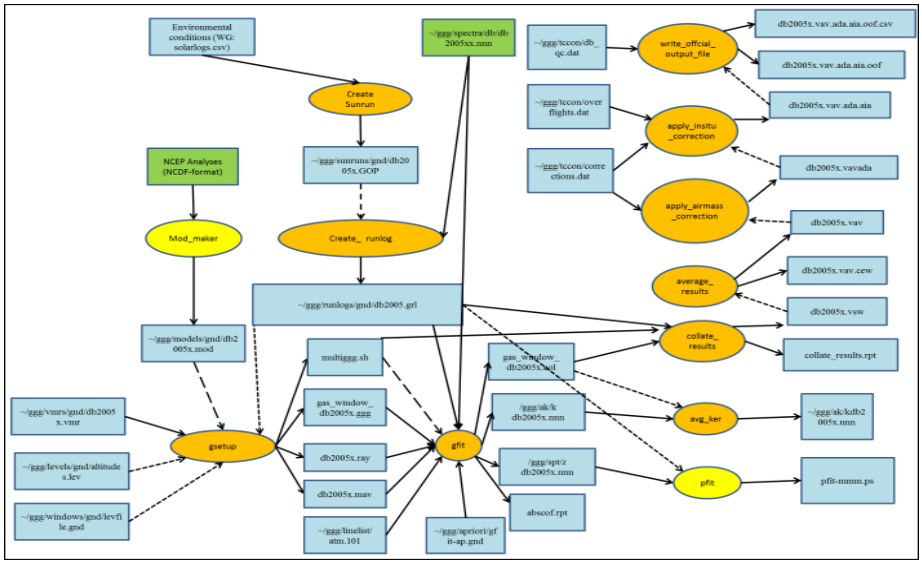

Figure 7: Schematic views of the TCCON GGG2014 standard retrieval software.

2.6 OCO-2

Orbiting Carbon Observatory-2 (OCO-2) is NASA's first Earth-orbiting satellite, which was successfully launched on July 2, 2014 into low-Earth orbit. It is devoted to observing atmospheric carbon dioxide (CO_2) to get better insight for the carbon cycle. The primary mission is to measure carbon dioxide with high precision and accuracy in order to characterize its sources and sinks at different spatial and temporal scales (Boland et al., 2009; Crisp, 2008, 2015). The instrument measures the near infrared spectra (NIR) of sunlight reflected off the Earth's surface. Using a retrieval algorithm, it provides results of atmospheric abundances of carbon dioxide and related atmospheric parameters at

the nadir, sun glint and targets modes. Detailed information about the instrument is available in different papers (Connor et al., 2008; O'Dell et al., 2012). In this work, we used the OCO-2 version 7Br bias corrected data.

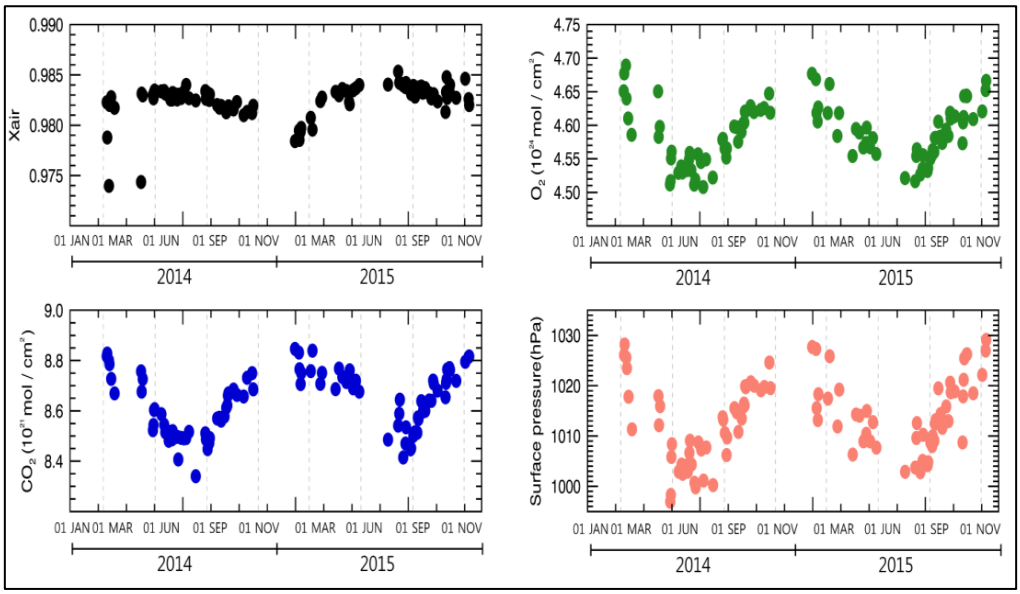

240 **Figure 8**: Time series of X_{air} (top left panel), total column amounts of CO_2 (bottom left panel), total column amounts of O_2 (top right panel), and surface pressure (pout) (bottom right panel) from the g-b FTS are depicted during 2014- 2015.

3 Results and discussion

3.1 Time series of X_{air} and columns of CO_2 and O_2

245 The time series of column-averaged abundance of dry air (X_{air}) is given in the top left panel of Fig. 8. It shows that the values of X_{air} are fluctuated between 0.974 and 0.985, and the mean value is 0.982 with a standard deviation of 0.0015 in which the scatter for X_{air} is about 0.15 %. The low variability in time series of X_{air} indicates the stability of the measurements. The temporal distributions of the g-b FTS total column amounts of CO_2 and O_2 on daily mean basis during the period from February 2014 to December 250 2015 are depicted in the left bottom and right top panels of Fig. 8, respectively. It was shown that the CO_2 column amounts varied within 8.40×10^{21} to 8.84×10^{21} molecules cm^{-2} during the whole observation period, while O_2 varied between 4.5×10^{24} and 4.7×10^{24} molecules cm^{-2}, with the corresponding mean of 4.52×10^{24} molecules cm^{-2} and a standard deviation of 2.59×10^{22} molecules cm^{-2}, respectively. The scatter for column O_2 is estimated to be 0.57 %, which is comparable with the 255 variation of atmospheric pressure (see Fig. 8 right top and bottom panels).

3.2 Comparison of the daily average XCO_2 between the g-b FTS and OCO-2

In this section, we present a comparison of XCO_2 between the g-b FTS and OCO-2 version 7Br data (bias corrected data) over Anmyeondo station during the period between 2014 and 2015. For making a comparison of the g-b FTS measurements, we applied the spatial coincidence criteria for the OCO-2 260 data over land within 4° latitude/longitude of the FTS station, as well as setting up a time window of 1

day. In addition, a direct comparison was made between the g-b FTS and OCO-2, without considering the effects of different apriori profiles and averaging kernels since we do not have CO_2 profile that reflects the actual variability over the measurement site. Based on the coincidence criteria, we obtained nine coincident measurements, which were not sufficient to infer a robust conclusion. But it gives a preliminary result for indicating a level of agreement between them. We showed that the comparison of the time series on daily mean basis of XCO_2 concentrations derived from the g-b FTS and OCO-2 along with the time series of its retrieval errors from FTS during the measurement period between 2014 and 2015, as depicted in Fig. 9. As can be seen in the plot, the g-b FTS measurement exhibits some gaps occurred due to bad weather conditions, instrument failures, and absences of an instrument operator. In the present analysis, the XCO_2 concentrations from FTS were considered only when its retrieval error was below 1.5 ppm (see the bottom panel of Figure 8), which is the sum of all error components such as laser sampling error, zero level offsets, ILS error, smoothing error, atmospheric apriori temperature, atmospheric apriori pressure, surface pressure, and random noise. Recently, Wunch et al. (2016) reported that the comparison of XCO_2 derived from the OCO-2 version 7Br data against a co-located ground-based TCCON data that indicates the median differences between the OCO-2 and TCCON data were less than 0.5 ppm, a corresponding RMS differences less than 1.5 ppm. The overall results of our comparisons are comparable with the report made by Wunch et al. (2016). The OCO-2 product of XCO_2 was biased (satellite minus g-b FTS) with respect to the g-b FTS, which was lowered by 0.065 ppm with a standard deviation of 1.66 ppm. This bias could be attributed to the instrument uncertainty. In addition to that, we also obtained a strong correlation between them, which was quantified as a correlation coefficient of 0.85 (see Table 4).

Table 4. Summary of the statistics of XCO_2 comparisons between OCO-2 and the g-b FTS from 2014 to 2015 are presented. N–coincident number of data, R-correlation coefficient, RMSE - Root Mean Squares Error.

N	Abso. diff. (ppm)	Rel. diff (%)	R	RMSE (ppm)
9	-0.065±1.665	-0.0167±0.418	0.854	1.571

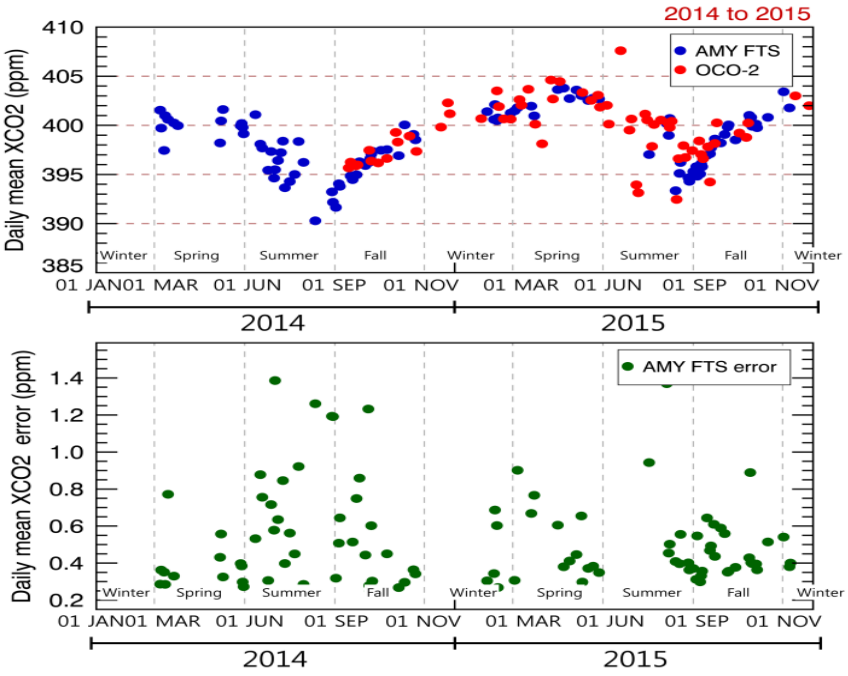

Figure 9: Top Panel: The time series of XCO_2 from the g-b FTS (blue dot) and OCO-2 (red dot) over the Anmyeondo site from 2014 to 2015. Bottom panel: The time series of FTS XCO_2 errors. All results are given on daily mean basis.

3.3 Comparison of seasonal cycle of XCO_2

In this section, the main focus of this issue is to deal with the comparison of the seasonal cycle of XCO_2 between the g-b FTS and OCO-2 over the Anmyeondo station. The top panel of Fig. 9 exhibits the time series of the daily mean XCO_2 from 2014 to 2015. The overall result indicates that both instruments are generally agreed in capturing the seasonal variability of XCO_2 at the measurement site. As it is clearly seen from the temporal distribution of FTS XCO_2, the maximum and minimum values are observed in spring and late summer seasons, respectively. It was found that its mean values in spring and summer were 402.63 and 396.58 ppm, respectively (see Table 5). This is because the seasonal variation of XCO_2 is controlled mainly by the photosynthesis in the terrestrial ecosystem, and this explains the larger XCO_2 values in the northern hemisphere in late April (Schneising et al. 2008, and references therein). The minimum value of XCO_2 occurs in August due to uptake of carbon into the biosphere, which is associated with the period of plant growth. Furthermore, both instruments showed high standard deviations during summer, about 2.56 ppm in FTS and 3.41 ppm in OCO-2, suggesting that the variability reflects strong sources and sink signals.

Table 5. Seasonal mean and standard deviations of XCO_2 from the g-b FTS and OCO-2 in the period between 2014 and 2015 are given below.

Season	g-b FTS XCO_2 mean ± std (ppm)	OCO-2 XCO_2 mean ± std (ppm)
Winter	401.01 ± 0.62	401.57 ± 1.17
Spring	402.63 ± 0.87	402.43 ± 1.81
Summer	396.58 ± 2.56	398.94 ± 3.41
Fall	398.62 ± 2.21	397.49 ± 1.58

4 Conclusions

Monitoring of greenhouse gases is an essential issue in the context of the global climate change. Accurate and precise continuous long-term measurements of the greenhouse gases (GHGs) are substantial for investigating their source and sinks. Nowadays, several remote sensing instruments operated on different platforms are dedicated for measuring GHGs.

XCO_2 measurements have been made using the g-b FTS at the Anmyeondo site since 2013. However, in this work, we focused on the measurements taken during 2014 and 2015. The instrument has been operated in a semi-automated mode since then. The FTS instrument has been stable during the whole measurement period. Regular instrument alignments using the HCl cell measurements are performed. The other important feature is that the home made OASIS system is installed in our FTS instrument, which enables to improve the solar intensity fluctuations. Thus, it guarantees the quality of the spectra. The TCCON standard GGG2014 retrieval software is used to retrieve XCO_2 from the g-b FTS spectra.

In this work, the preliminary comparison results of XCO_2 between FTS and OCO-2 were presented over the Anmyeondo station. The mean absolute difference of XCO_2 between FTS and OCO-2 was calculated on daily mean basis, and it was estimated to be -0.065 ppm, along with a standard deviation of 1.67 with respect to the g-b FTS. This bias could be attributed with instrument uncertainty. Based on the seasonal cycle comparison, both the g-b FTS and OCO-2 illustrated a consistent pattern in capturing the seasonal variability of XCO_2, with maximum in spring and minimum in summer. In summer and fall, plants are flourishing and CO_2 is consumed by photosynthesis. However, in winter and spring, weak photosynthesis phenomenon is occurred because of low plant flourishing and CO_2 reaches the highest values particularly in April. Therefore, the outcome of this study reflects the suitability of the measurements for improving the understanding of the carbon cycle, as well as for evaluating the remote sensing data.

5 Acknowledgements

This research was supported by the Research and Development for KMA Weather, Climate, and Earth system Services (NIMS-2016-3100).

References

Boland, S., Brown L. R., Burrows J. P., Ciais P., Connor B. J., Crisp D., Denning S., Doney S. C., Engelen R., Fung I. Y., Griffith P., Jacob D. J., Johnson B., Martin-Torres J., Michalak A. M., Miller C. E., Polonsky I., Potter C., Randerson J. T., Rayner P. J., Salawitch R. J., Santee M., Tans P. P., Wennberg P. O., Wunch D., Wofsy S. C., and Yung Y. L.: The Need for Atmospheric Carbon

Dioxide Measurements from Space: Contributions from a Rapid Reflight of the Orbiting Carbon Observatory, 2009, http://www.nasa.gov/pdf/363474main_OCO_Reflight.pdf.

Buschmann M., Nicholas M., Deutscher M., Sherlock V., Palm M., Warneke T., and Notholt J.: Retrieval of XCO2 from ground-based mid-infrared (NDACC) solar absorption spectra and comparison to TCCON, Atmos. Meas. Tech., 9, 577–585, 2016.

Brault, J. W.: New approach to high-precision Fourier transform spectrometer design. Appl. Opt. 35, 2891–2896, 1996.

Connor B. J., Bösch H., Toon G., Sen B., Miller C. E., and Crisp D.: Orbiting carbon observatory: Inverse method and prospective error analysis, J. Geophys. Res., 113 doi: 10.1029/2006JD008336, 2008.

Connor B. J., Sherlock V., Toon G., Wunch D., and Wennberg P. O.: GFIT2: an experimental algorithm for vertical profile retrieval from near-IR spectra, Atmos. Meas. Tech., 9(8), 3513–3525, doi:10.5194/amt-9-3513-2016, 2016.

Crisp D., Miller C. E., DeCola P. L.: NASA Orbiting Carbon Observatory: measuring the column averaged carbon dioxide mole fraction from space. J. Appl. Remote Sens., 2, 023508, doi:10.1117/1.2898457, 2008.

Crisp D. for the OCO-2 Team: Measuring Atmospheric Carbon Dioxide from Space with the Orbiting Carbon Observatory-2 (OCO-2), Proc. SPIE 9607, Earth Observing Systems XX, 960702, doi: 10.1117/12.2187291, 2015.

Deutscher, N. M., Griffith, D. W. T., Bryant, G. W., Wennberg, P. O., Toon, G. C., Washenfelder, R. A., Keppel-Aleks, G., Wunch, D., Yavin, Y., Allen N. T., Blavier, J.-F., Jiménez R., Daube, B. C., Bright, A. V., Matross, D. M., Wofsy, S. C., and Park, S.: Total column CO2 measurements at Darwin, Australia-site description and calibration against in situ aircraft profiles, Atmos. Meas. Tech., 3, 947-958, doi:10.5194/amt-3-947-2010, 2010.

Frankenberg, C., Pollock, R., Lee, R. A. M., Rosenberg, R., Blavier, J.-F., Crisp, D., O'Dell C. W., Osterman, G. B., Roehl, C., Wennberg, P. O., and Wunch, D.: The Orbiting Carbon Observatory (OCO-2): spectrometer performance evaluation using pre-launch direct sun measurements. Atmospheric Measurement Techniques, 8(1), 301–313. doi:10.5194/amt-8-301-2015, 2015.

Geibel, M. C., Gerbig, C., and Feist, D. G.: A new fully automated FTIR system for total column measurements of greenhouse gases, Atmospheric Measurement Techniques, 3(5), 1363-1375, doi:10.5194/amt-3-1363-2010, 2010.

Hase, F., Blumenstock, T., and Paton-Walsh, C.: Analysis of the instrumental line shape of high resolution Fourier transform IR spectrometers with gas cell measurements and new retrieval software, Appl. Optics, 38, 3417–3422, doi:10.1364/AO.38.003417,1999.

Hase, F., Drouin, B. J., Roehl C. M., Toon, G. C., Wennberg, P. O., Wunch, D., Blumenstock, T., Desmet F., Feist, D. G., Heikkinen, P., De Mazière, M., Rettinger, M., Robinson, J., Schneider, M.,

Sherlock, V., Sussmann, R., Té Y., Warneke, T., and Weinzierl, C.: Calibration of sealed HCl cells used for TCCON instrumental line shape monitoring, Atmospheric Measurement Techniques, 6(12), 3527–3537, doi:10.5194/amt-6-3527-2013, 2013.

Kiel, M., Wunch, D., Wennberg, P. O., Toon, G. C., Hase, F., and Blumenstock, T.: Improved retrieval of gas abundances from near-infrared solar FTIR spectra measured at the Karlsruhe TCCON station, Atmos. Meas. Tech., 9(2), 669–682, doi:10.5194/amt-9-669-2016, 2016.

Kivi, R. and Heikkinen, P.: Fourier transform spectrometer measurements of column CO2 at Sodankylä, Finland, Geosci. Instrum. Method. Data Syst., 5, 271–279, 2016.

Messerschmidt, J., Macatangay, R., Notholt, J., Petri C., Warneke, T., and Weinzierl, C.: Side by side measurements of CO2 by ground-based Fourier transform spectrometry (FTS), Tellus B, 62(5), 749-758, doi:10.1111/j.1600-0889.2010.00491.x., 2010.

Messerschmidt, J., H. Chen, N. M. Deutscher, C. Gerbig, P. Grupe, K. Katrynski, F.-T. Koch, J. V. Lavrič, J. Notholt, C. Rödenbeck, W. Ruhe, T. Warneke, and Weinzierl, C.: Automated ground-based remote sensing measurements of greenhouse gases at the Białystok site in comparison with collocated in situ measurements and model data, Atmospheric Chemistry and Physics, 12(15), 6741–6755, doi:10.5194/acp-12-6741-2012, 2012.

Miao, R., Lu N., Yao L., Zhu, Y., Wang, J., and Sun, J.: Multi-Year Comparison of Carbon Dioxide from Satellite Data with Ground-Based FTS Measurements (2003–2011), Remote Sensing, 5(7), 3431–3456, doi:10.3390/rs5073431, 2013.

Miller, C. E., Crisp, D. DeCola, P. L., Olsen, S. C., Randerson, J. T., Michalak, A. M., Alkhaled, A., Rayner, P., Jacob, D. J., Suntharalingam, P., Jones, D. B. A., Denning, A. S., Nicholls, M. E., Doney, S. C., Pawson, S., Boesch, H., Connor B. J., Fung I. Y., O'Brien, D., Salawitch, R. J., Sander, S. P., Sen, B., Tans, P., Toon, G. C., Wennberg, P. O., Wofsy, S. C., Yung, Y. L., and Law, R. M.: Precision requirements for space-based XCO2 data, J. Geophys. Res-Atmos., 109, D02301, doi: 10.1029/2006JD007659, 2007.

Morino, I., Uchino, O., Inoue, M., Yoshida, Y., Yokota T., Wennberg, P. O., Toon, G. C., Wunch, D., Roehl, C. M., Notholt, J., Warneke, T., Messerschmidt, J., Griffith, D. W. T., Deutscher, N. M., Sherlock, V., Connor, B. J., Robinson, J., Sussmann, R., and Rettinger, M.: Preliminary validation of column-averaged volume mixing ratios of carbon dioxide and methane retrieved from GOSAT short-wavelength infrared spectra, Atmospheric Measurement Techniques, 4(6), 1061-1076, doi:10.5194/amt-4-1061-2011, 2011.

O'Dell, C. W., Connor, B., Bösch, H., O'Brien, D., Frankenberg C., Castano, R., Christi, M., Eldering, D., Fisher, B., Gunson, M., McDuffie, J., Miller, C. E., Natraj, V., Oyafuso, F., Polonsky, I., Smyth, M., Taylor, T., Toon, G. C., Wennberg, P. O., and Wunch, D.: The ACOS CO2 retrieval algorithm – Part 1: Description and validation against synthetic observations, Atmospheric Measurement

Techniques, 5, 99–121, doi: 10.5194/amt-5-99-2012, http://www.atmos-meas-tech.net/5/99/2012/, 2012.

Ohyama, H., Morino, I., Nagahama, T., Machida, T., Suto H., Oguma, H., Sawa, Y., Matsueda, H., Sugimoto, N., Nakane, H., and Nakagawa, K.: Column-averaged volume mixing ratio of CO2 measured with ground-based Fourier transform spectrometer at Tsukuba, J. Geophys. Res., 114, D18303 doi:10.1029/2008JD011465, 2009.

Ohyama, H., Kawakami, S., Tanaka, T., Morino, Uchino, I., O., Inoue, M., Sakai, T., Nagai, T., Yamazaki, A., Uchiyama, A., Fukamachi, T., Sakashita, M., Kawasaki, T., Akaho, T., Arai, K., and Okumura, H.: Observations of XCO2 and XCH4 with ground-based high-resolution FTS at Saga, Japan, and comparisons with GOSAT products, Atmos. Meas. Tech., 8(12), 5263–5276, doi:10.5194/amt-8-5263-2015..

Rayner P. J., and O'Brien D. M.: The utility of remotely sensed CO2 concentration data in surface source inversions, Geophys. Res. Lett., 28, 175–178, doi: 10.1029/2000GL011912, 2001.

Rothman et al. (2013). The HITRAN 2012 Molecular Spectroscopic Database, J. Quant. Spectrosc. Ra., Elsevier, ISSN 0022-4073.

Schneising O., Buchwitz M., Burrows J. P., Bovensmann H., Reuter M., Notholt J., Macatangay R., and Warneke T.: Three years of greenhouse gas column-averaged dry air mole fractions retrieved from satellite-Part 1: Carbon dioxide, Atmos. Chem. Phys., 8, 3827-3853, 2008.

Sun, Y., Palm, M., Weinzierl, C., Peteri, C., Notholt, J., Wang, Y., and Liu C.: Technical note: Sensitivity of instrumental line shape monitoring for the ground-based high-resolution FTIR spectrometer with respect to different optical attenuators, Atmos. Meas. Tech. Discuss., doi:10.5194/amt-10-989- 2017.

Washenfelder R. A., Toon G. C., Blavier J-F., Yang Z., Allen N. T., Wennberg P. O., Vay S. A., Matross D. M., and Daube B. C.: Carbon dioxide column abundances at the Wisconsin Tall Tower site, Journal of Geophysical Research, 2006, 111, doi:10.1029/2006JD00715, 2000. Warneke, T., Yang, Z., Olsen, S., Korner, S., Notholt J., Toon, G. C., Velazco, V., Schultz, A., and Schrems, O.: Seasonal and latitudinal variations of column averaged volume-mixing ratios of atmospheric CO2, Geophysical Research Letters, 32(3), 2-5, doi:10.1029/2004GL021597, 2005.

Wunch, D., Toon G. C., Wennberg, P. O., Wofsy, S. C., Stephens, B., Fisher, M. L., Uchino O., Abshire, J. B., Bernath, P. F., Biraud, S. C., Blavier J.-F. L., Boone, C. D., Bowman, K. P., Browell, E. V., Campos, T., Connor, B. J., Daube, B. C., Deutscher, N. M., Diao M., Elkins J. W., Gerbig C., Gottlieb E., Griffith, D. W. T., Hurst, D. F., Jiménez, R., Keppel-Aleks G., Kort E. A., Macatangay R., Machida T., Matsueda, H., Moore F. L., Morino I., Park S., Robinson J., Roehl C. M., Sawa Y., Sherlock V., Sweeney C., Tanaka T., and Zondlo M. A.: Calibration of the Total Carbon Column Observing Network using aircraft profile data, Atmospheric Measurement Techniques, 3(5), 1351-1362, doi:10.5194/amt-3-1351-2010.

Wunch, D., Toon, G. C., Blavier, J.-F. L., Washenfelder, R. A., Notholt, J., Connor, B. J., Griffith, D. W. T., Sherlock V., and Wennberg P. O.: The Total Carbon Column Observing Network, Philos. T. R. Soc. A, 369, 2087–2112, doi:10.1098/rsta.2010.0240, 2011.

Wunch, D., Toon G. C., Sherlock V., Deutscher N. M., Liu X., Feist D. G., and Wennberg P. O.: The Total Carbon Column Observing Network's GGG2014 Data Version. doi:10.14291/tccon.ggg2014.documentation.R0/1221662, 2015.

Wunch, D., Wennberg, P.O.,, Osterman, G., Fisher, B.,Naylor, B.,, Roehl, C. M., O'Dell, C., Mandrake, L.,Viatte, C., Griffith, D. W. T., Deutscher, N. M., Velazco, V. A., Notholt, J.,Warneke, T.,Petri, C., Maziere, M. De, Sha, M. K., Sussmann,R., Rettinger, M., Pollard, D., Robinson, J.,Morino, I., Uchino O.,Hase, F., Blumenstock, T., Kiel, M., Feist, D. G., Arnold S.G., Strong, K., Mendonca, J., Kivi, R.,Heikkinen, P., Iraci, L., Podolske, J., Hillyard, P. W., Kawakami, S., Dubey, M. K., Parker, H. A., Sepulveda, E., Rodriguez, O. E. G., Te, Y., Jeseck, P., Gunson, M. R., Crisp, D., and Eldering A., Comparisons of the Orbiting Carbon Observatory-2 (OCO-2) XCO2 measurements with TCCON, Atmos. Meas. Tech. Discuss., doi:10.5194/amt-2016-227, 2016.